

Hsp90 inhibitor PU-H71, a multimodal inhibitor of malignancy, induces complete responses in triple-negative breast cancer models

Eloisi Caldas-Lopes^a, Leandro Cerchietti^b, James H. Ahn^a, Cristina C. Clement^a, Ana I. Robles^c, Anna Rodina^a, Kamalika Moulick^a, Tony Taldone^a, Alexander Gozman^a, Yunke Guo^a, Nian Wu^a, Elisa de Stanchina^a, Julie White^a, Steven S. Gross^b, Yuliang Ma^b, Lyuba Varticovski^c, Ari Melnick^b, and Gabriela Chiosis^{a,1}

^aProgram in Molecular Pharmacology and Chemistry and Department of Medicine, Memorial Sloan-Kettering Cancer Center, New York, NY 10021; ^bDepartment of Medicine, Division of Hematology and Medical Oncology, and Department of Pharmacology, Weill Cornell Medical College, New York, NY 10065; and ^cLaboratory of Human Carcinogenesis, Center for Cancer Research, National Cancer Institute, National Institutes of Health, Bethesda, MD 20892

Communicated by Samuel J. Danishefsky, Memorial Sloan-Kettering Cancer Center, New York, NY, March 27, 2009 (received for review January 22, 2009)

Triple-negative breast cancers (TNBCs) are defined by a lack of expression of estrogen, progesterone, and HER2 receptors. Because of the absence of identified targets and targeted therapies, and due to a heterogeneous molecular presentation, treatment guidelines for patients with TNBC include only conventional chemotherapy. Such treatment, while effective for some, leaves others with high rates of early relapse and is not curative for any patient with metastatic disease. Here, we demonstrate that these tumors are sensitive to the heat shock protein 90 (Hsp90) inhibitor PU-H71. Potent and durable anti-tumor effects in TNBC xenografts, including complete response and tumor regression, without toxicity to the host are achieved with this agent. Notably, TNBC tumors respond to retreatment with PU-H71 for several cycles extending for over 5 months without evidence of resistance or toxicity. Through a proteomics approach, we show that multiple oncoproteins involved in tumor proliferation, survival, and invasive potential are in complex with PU-H71-bound Hsp90 in TNBC. PU-H71 induces efficient and sustained downregulation and inactivation, both *in vitro* and *in vivo*, of these proteins. Among them, we identify downregulation of components of the Ras/Raf/MAPK pathway and G₂-M phase to contribute to its anti-proliferative effect, degradation of activated Akt and Bcl-xL to induce apoptosis, and inhibition of activated NF- κ B, Akt, ERK2, Tyk2, and PKC to reduce TNBC invasive potential. The results identify Hsp90 as a critical and multimodal target in this most difficult to treat breast cancer subtype and support the use of the Hsp90 inhibitor PU-H71 for clinical trials involving patients with TNBC.

targeted therapy | triple-negative breast tumors | heat shock protein 90 | purine-scaffold Hsp90 inhibitor PU-H71 | basal-like breast cancer

TNBC accounts for 15% of breast tumors and for a higher percentage of breast cancer in African and African-American women who are premenopausal (1, 2). Histologically, triple-negative breast cancers (TNBCs) are poorly differentiated, and most fall into the basal subgroup of breast cancers, as defined by gene expression profiling (1, 3). Recently, it has been shown that women carrying breast cancer gene 1 (BRCA1) mutations are more likely to develop TNBCs with a basal-like phenotype (4). The absence of tumor-specific treatment options in this cancer subset underscores the critical need to develop a better understanding of the biology of this disease, as well as to advance treatment strategies for these patients (1, 3).

Heat shock protein 90 (Hsp90) is a molecular chaperone protein that is widely expressed in breast cancer (5). Its ability to stabilize client oncogenic proteins suggests a crucial role for Hsp90 in maintaining the survival of breast cancer cells. Along these lines, Hsp90 can maintain a large pool of active and folded oncoproteins, for which its activated form has particular affinity and, as such, can serve as a protective “biochemical buffer” for cancer causing oncogenes (6). In this respect, degradation of a specific Hsp90 client in the appropriate genetic context [e.g., BRAF in a melanoma cell

with V600E mutant BRAF or overexpressed HER2 in a HER2-overexpressing (HER2⁺) breast tumor] results in apoptosis and/or differentiation, whereas client protein degradation in normal cells, has little or no effect. This ability to interact and chaperone a large number of client oncogenic kinases and transcription factors has led to the clinical development of Hsp90 inhibitors in a broad range of tumors (6).

In breast cancer, preclinical studies have demonstrated a notable sensitivity of HER2⁺ tumors to Hsp90 inhibitors (6). In addition, first generation of geldanamycin-based Hsp90 inhibitors, 17-AAG (also called Tanespimycin, KOS-953, and IPI-504) and 17-DMAG (alvespimycin, KOS-1022) (Fig. S1a) were clinically developed for this subset and demonstrated responses even (and in particular) in patients with progressive disease after trastuzumab therapy (7). TNBC tumors however, are more resistant to the action of these agents (8–10). One interpretation of these findings is that Hsp90 may not be as crucial for maintaining the malignant phenotype in TNBC, or alternatively, Hsp90-oncoproteins essential in TNBC may not be efficiently downregulated by doses of Hsp90 inhibitors that can be safely administered *in vivo*. These interpretations suggest that TNBC patients would not receive clinical benefit from treatment with Hsp90 inhibitors.

Contrary to this view, we present here our current findings to demonstrate that TNBCs, similarly to HER2⁺ tumors, are sensitive to Hsp90 inhibition not only *in vitro* but also in preclinical *in vivo* models. Our findings demonstrate that TNBC tumors rely strongly on Hsp90 chaperoning for their proliferative, survival, metastatic, and anti-apoptotic potential, establishing Hsp90 as an effective and pluripotent target for therapy of TNBC.

Results and Discussion

PU-H71 Potently Suppresses the Growth of TNBC Cells and Induces Significant Killing of the Initial Cancer Cell Population. To investigate the role of Hsp90 in TNBC, we made use of the novel Hsp90 inhibitor PU-H71 (Fig. S1a), currently in late-stage IND evaluation (11). The cytotoxic effect of PU-H71 in the TNBC cell lines MDA-MB-468, MDA-MB-231, and HCC-1806 was determined using an assay that estimates ATP levels. PU-H71 potently repressed growth at concentrations that bind Hsp90 in these cells (Fig. 1a and Fig. S1b and c). In addition, PU-H71 induced significant cytotoxicity; after 72 h incubation with a concentration

Author contributions: E.C.-L., L.C., C.C.C., A.I.R., A.R., N.W., E.d.S., J.W., S.S.G., A.M., and G.C. designed research; E.C.-L., L.C., J.H.A., C.C.C., A.I.R., A.R., K.M., A.G., Y.G., N.W., E.d.S., J.W., and Y.M. performed research; L.C. and T.T. contributed new reagents/analytic tools; E.C.-L., L.C., A.R., S.S.G., Y.M., L.V., and G.C. analyzed data; and E.C.-L., L.C., A.R., L.V., A.M., and G.C. wrote the paper.

The authors declare no conflict of interest.

¹To whom correspondence should be addressed. E-mail: chiosisg@mskcc.org.

This article contains supporting information online at www.pnas.org/cgi/content/full/0903392106/DCSupplemental.

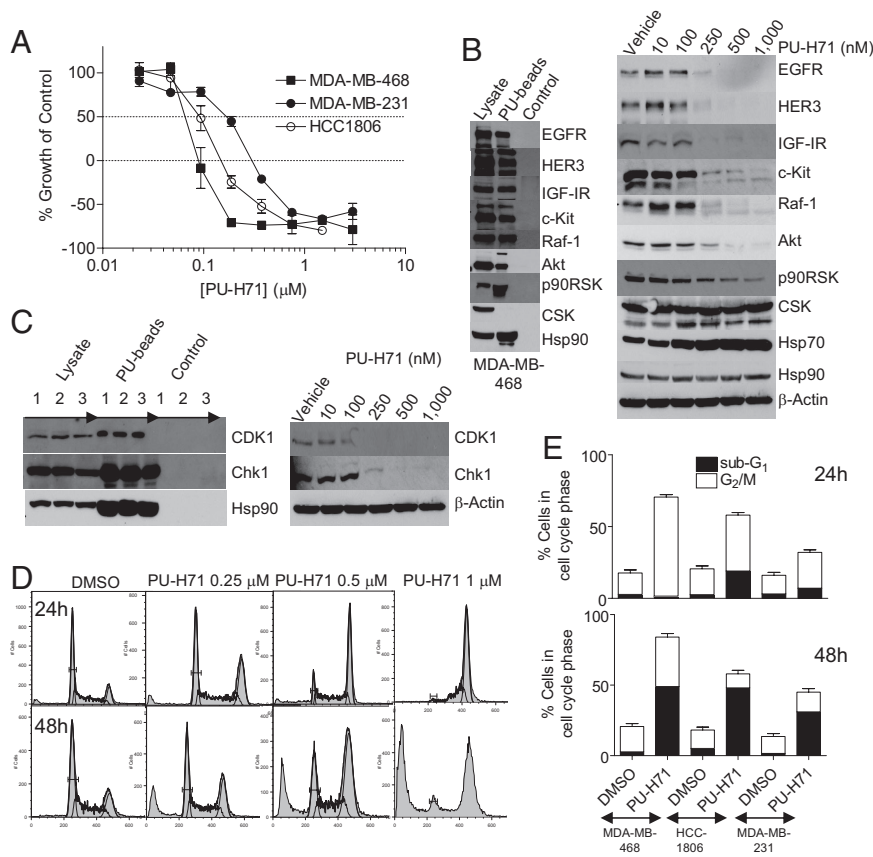


Fig. 1. PU-H71 inhibits cell proliferation and blocks TNBC cells in G₂-M. (A) Representative TNBC cells were incubated with increasing concentrations of PU-H71 and growth over 72 h was assessed. y-axis values below 0% represent cell death of the starting population. (B and C, Left) Hsp90-containing protein complexes isolated through chemical precipitation with beads having attached PU-H71 (PU-beads) or an Hsp90-inert molecule (control) were analyzed by western blot. Lysate, endogenous protein content; 1, MDA-MB-468; 2, MDA-MB-231; and 3, HCC-1806 cells. (Right) MDA-MB-468 cells were treated for 24 h with indicated concentrations of PU-H71, and protein extracts were analyzed by western blot. (D) MDA-MB-468 cells were treated for 24 h (Upper) or 48 h (Lower) with vehicle or with the indicated concentrations of PU-H71. DNA content was analyzed by propidium iodide staining and flow cytometry. (E) TNBC cells were treated for 24 h (Upper) or 48 h (Lower) with vehicle or PU-H71 (1 μM). The fraction of cells in G₂-M and subG₁ was analyzed by flow cytometry, quantified in FlowJo, and data were graphed.

of PU-H71 (1 μM) that is 5- to 10-times higher than its IC₅₀ for growth inhibition (Fig. S1*b* and *c*), PU-H71 killed 80%, 65%, and 80% of the initial population of MDA-MB-468, MDA-MB-231, and HCC-1806 cells, respectively (Fig. 1*A*).

The natural product derivatives 17-AAG and 17-DMAG, and the unrelated purine-scaffold compound CNF-2024 (renamed BIIB021) (Fig. S1*a*), bound Hsp90 extracted from TNBC cells with a similar low nanomolar affinity (Fig. S1*b*). Aside for 17-AAG, all compounds inhibited cell growth and induced comparable cell killing at concentrations in agreement with their Hsp90 affinity (Fig. S1*c*), suggesting *in vitro* a common, Hsp90-mediated, mechanism of action for these chemically distinct drugs.

These findings rank TNBC cells, relative to certain HER2⁺ breast cancer cells, as most sensitive to killing by an Hsp90 inhibitor (Fig. S2*a* and *b*). In ER⁺ and a low number of HER2⁺ breast cancer cells, although Hsp90 inhibition induced potent suppression of cell growth and degradation of Hsp90 onco-clients (Fig. S2*e* and *f*), it was associated with a limited cytotoxic effect (Fig. S2*a* and *b*), suggestive of a prevalent cytostatic mechanism of action.

PU-H71 Leads to Downregulation of Oncoproteins Involved in Driving the Enhanced Proliferation of TNBCs. TNBC tumors express several receptors, such as the epidermal growth factor receptor (EGFR), insulin-like growth-factor receptor (IGF1R), HER3, and c-Kit, demonstrated to augment their proliferative potential through activation of the Ras/Raf/MEK/ERK pathway (1, 3). HER3 also plays a critical role in EGFR-driven tumors (12) and was directly implicated in the proliferation and migration of MDA-MB-468 cells (13). We found a multitude of these components, such as EGFR, IGF1R, HER3, c-Kit, and Raf-1, forming a complex with PU-H71-bound Hsp90 (Fig. 1*B*, Left). We also identified Raf/MEK/ERK pathway components never before reported to be Hsp90 bound, such as p-ERK2 and p90RSK (Fig. S3). It is generally accepted that

in tumors, many malignancy driving molecules are chaperoned by Hsp90, which acts as a biochemical buffer allowing for the existence of cancer phenotypes (6). When Hsp90 becomes inactivated, these tumor-driving proteins become destabilized and are subsequently degraded, mainly by the proteasome machinery (6). Concordantly, Hsp90 inhibition by PU-H71 induced a dose-dependent degradation or inactivation of these tumor driving molecules (Fig. 1*B*, Right and Fig. S4), suggesting that the anti-proliferative effect of PU-H71 is a direct consequence of depleting the TNBC cells of these proliferation-driving molecules.

CSK, a non-oncogenic c-Src related tyrosine kinase, was not identified in the PU-H71-Hsp90-pulldowns (Fig. 1*B*, Left) and accordingly, its levels remained unaffected by the inhibitor (Fig. 1*B*, Right). In all cases, β-actin or phosphatidylinositol-3 kinase (PI3K) p85 subunit, proteins of whose levels are insensitive to Hsp90 inhibition (6), were used as a protein loading control.

Inhibition of Proliferation in TNBC Cells Is Associated with a G₂-M Block Arrest. We find that in TNBC, Hsp90 is also in complex with cell cycle regulatory proteins such as cyclin-dependent kinase 1 (CDK1) and checkpoint kinase 1 (Chk1) (Fig. 1*C*, Left), proteins essential for G₂-M progression (14). PU-H71 led to a reduction in their levels (Fig. 1*C*, Right). Because inhibition of CDK1 is sufficient to result in a G₂-M block (14), we investigated the effects of PU-H71 on cell cycle. TNBC cells were treated with increasing concentrations of PU-H71 (Fig. 1*D* and Figs. S5*a* and *c*). Vehicle only treated MDA-MB-468 cells show a typical pattern of randomly cycling cells distributed across the G₁ (50%), S (35%), and G₂-M (17%) phases, at 24 and 48 h. Treatment for 24 h with 0.25, 0.5, and 1 μM PU-H71, augmented the percent of cells in G₂-M phase to 30%, 44%, and 69%, respectively (Fig. 1*D*, Upper). By 48 h, these decreased to 22%, 37%, and 35%, respectively, but were associated with an increased hypodiploid (subG₁) population (18%, 31%, and 49%, respectively)

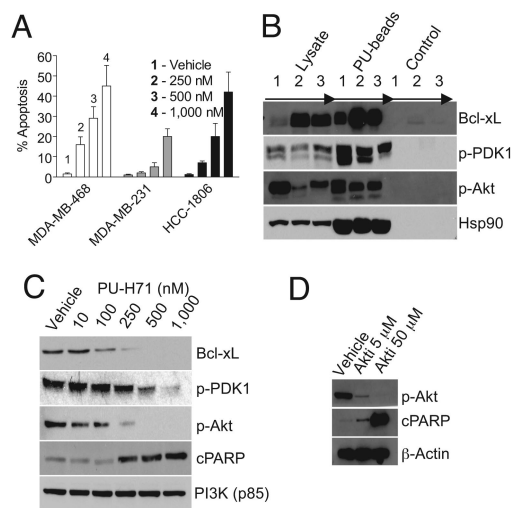


Fig. 2. PU-H71 induces significant apoptosis in TNBC. (A) TNBC cells were treated for 48 h with increasing concentrations of PU-H71. Cells were stained with Hoechst 33342 and YO-PRO-1. The number of cells exhibiting YO-PRO-1 fluorescence was counted, and positive cells (% apoptosis) were expressed as the ratio of YO-PRO-1-to-Hoechst 33342-positive cells \times 100. (B) Hsp90-containing protein complexes were isolated through chemical precipitation and analyzed as described. 1, MDA-MB-468; 2, MDA-MB-231; and 3, HCC-1806 cells. (C and D) MDA-MB-468 cells were treated for 24 h with vehicle and increasing concentrations of PU-H71 (C) or the Akt inhibitor (D), and protein extracts were subjected to immunoblotting.

(Fig. 1D, Lower). Similar dose-dependent G₂-M delay associated with a subsequent increase in cell death was observed for HCC-1806 and MDA-MB-231 cells (Fig. 1E and Fig. S5). Importantly, hypodiploid cells seem to derive from the G₂-M population, because the loss observed in the G₂-M peak was compensated by a similar gain in the subG₁ population, without change in other cell populations (Fig. 1D and E, and Figs. S5 and S6). In separate experiments, analysis of phospho-histone H3 levels, a marker of mitotic entry, indicated that the majority of cells collected in G₂-M at 24 h were actually in mitosis (Fig. S6b).

Whereas all tested Hsp90 inhibitors blocked TNBC cells in G₂-M, the kinetics and potency of cell cycle arrest and subsequent collapse into dead cells, were distinct among these agents, with PU-H71 and 17-DMAG most efficiently leading to cell death (Figs. S5 and S6).

PU-H71 Induces Apoptosis in TNBC, at Least in Part by Inactivation and Downregulation of Akt and Bcl-xL. To determine whether cell death was attributable to apoptosis, cells were treated with PU-H71, and effects on several effectors and mediators of apoptosis were analyzed (Fig. 2, and Figs. S2 and S7). In PU-H71-treated cells, there was a significant and preferential dose-dependent increase in YO-PRO-1-fluorescent cells (green) that demonstrate the morphological features of cells undergoing apoptosis, such as nuclear shrinkage and fragmentation (Fig. 2A and Fig. S7a), as well as of cells staining positive for annexin V and terminal deoxynucleotidyl transferase dUTP nick end labeling (TUNEL), indicative of early and late stage apoptosis, respectively (Fig. S2b). In addition, we observed a 2- to 4-fold increase in caspase-3 and -7 activities (Fig. S2c) at concentrations of this agent that were in agreement with its anti-proliferative activity (Fig. 1A). Caspase-3 activation by PU-H71 was concomitant with mitochondrial permeabilization (Fig. S2c) and cleavage of caspase-3 and PARP (cPARP; Fig. S2d), indicating sufficiency of this mechanism for PU-H71-triggered apoptosis.

The number of cells undergoing apoptosis (Fig. 2A) equaled the number of hypodiploid cells (Fig. 1E), suggesting that cell death upon Hsp90 inhibition by PU-H71 occurred mainly through apo-

ptosis. This hypothesis was confirmed when loss of viability by PU-H71 was attenuated by a pan-caspase inhibitor (Fig. S7b).

To understand mechanisms responsible for the potent apoptotic effect of PU-H71, we evaluated the effect of PU-H71 on several anti-apoptotic molecules, some of which are elevated in TNBC. Bcl-xL plays a role promoting survival of breast cancer cells in metastatic foci by counteracting the proapoptotic signals and favoring the successful development of metastases in a microenvironment of specific organs (15). It is also reported to play a role in protecting breast cancer cells from chemotherapy-provoked apoptosis, and downregulation of Bcl-xL is sufficient to induce apoptosis in TNBC cells and sensitize to killing by chemotherapy (16). We found that Bcl-xL is regulated by Hsp90 in TNBC cells (Fig. 2B). Along these lines and in accord with Hsp90 chaperoning, inhibition of Hsp90 by PU-H71 resulted in a substantial decrease of Bcl-xL total protein (Fig. 2C and Fig. S4), suggesting its degradation in response to PU-H71 contributive to apoptosis in TNBC cells.

In addition to this ubiquitous anti-apoptotic molecule, our findings implicated activated Akt as an important anti-apoptotic molecule in TNBC (Fig. 2 and Fig. S7c). Notably, activated Akt is expressed in most breast tumors and is associated with larger tumors, reduced tumor apoptosis, and abbreviated disease-free survival (17–19). The highest numbers of breast tumors with activated Akt are found in the triple-negative and the HER2⁺ breast cancer subtypes (18, 19). Moreover, reports also associate activation of Akt with tumors that evade the effects of anti-estrogen therapies (18). We found that inhibition of Akt alone in TNBC cells, using a specific small molecule inhibitor, is sufficient to induce apoptosis in TNBC cells (Fig. 2D and Fig. S7c). Activated Akt, as evidenced by phosphorylation at Ser-473 (17–19), as well as the Akt-activating kinase 3-phosphoinositide-dependent protein kinase-1 (PDK-1), were observed in complex with Hsp90 in TNBC cells (Fig. 2B) and are sensitive targets for degradation by PU-H71 (Fig. 2C and Fig. S4), suggesting the Akt survival pathway as an important target of PU-H71, and especially meaningful in reverting the anti-apoptotic phenotype in TNBCs. In contrast, we found that inhibition of key components of the Raf/MAPK/ERK, PKC α / β , and Jak-STAT pathways is insufficient to induce apoptosis of TNBC cells (Fig. S7d).

PU-H71 Leads to Downregulation of Oncoproteins Involved in the Invasive Potential of TNBCs. Another factor linked to hormone-independent breast cancer is nuclear factor- κ B (NF- κ B). NF- κ B activity is elevated in TNBC (20) and is implicated in enhanced cell survival, chemoresistance, and in the invasive and metastatic potential of these tumors (1, 3). Increased NF- κ B levels suppress apoptosis and induce epithelial-mesenchymal transitions (EMTs) (21). In TNBC, we identified several components of the NF- κ B pathway to be in complex with PU-H71-bound Hsp90. These are interleukin-1 receptor-associated kinase 1 (IRAK-1), TAK1-binding protein 2 and 3 (Tab2/3), and TBK1, also called NAK (NF- κ B-activated kinase) (Fig. S3). The IRAK/Tab complex recruits and activates TAK1, which directly phosphorylates IKK β at the activation loop to activate the IKK complex, resulting in NF- κ B activation (22). Concordantly, PU-H71 led to a proteasome-mediated reduction in IRAK-1 and TBK1 levels (Fig. 3A, Upper, and Fig. S3c), resulting in approximately 84% and 90% reduction in NF- κ B activity in MDA-MB-231 cells treated with 0.5 and 1 μ M PU-H71, respectively, compared with untreated control cells (Fig. 3A, Lower).

Another key signaling pathway that regulates tumor cell invasion is the PI3K/Akt pathway (17) and, concordantly, we find that an Akt inhibitor potentially inhibits the invasiveness of MDA-MB-231 (Fig. 3B).

In addition to Akt and NF- κ B, other proteins identified in PU-H71-bead pull-downs as Hsp90 clients in TNBC cells included the activated Janus kinase Tyk2, ERK1/2, and protein kinase C beta (PKC β) (Fig. S3); each of these interacting proteins are known to increase the invasiveness and metastatic potential of cancer cells

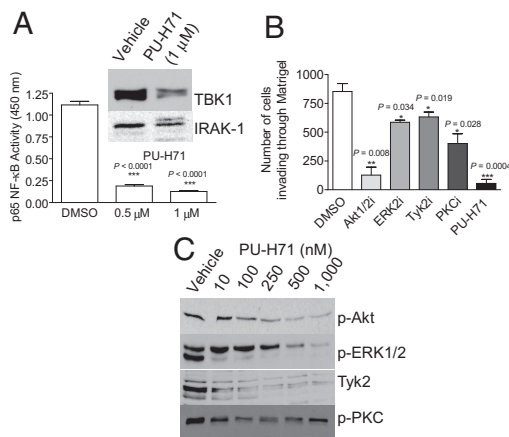


Fig. 3. PU-H71 inhibits invasion in TNBC cells. (A) MDA-MB-231 breast cancer cells were treated for 24 h with vehicle or the indicated concentrations of PU-H71. (Graph) Cells were collected, lysed, and then nuclear extracts were prepared for subsequent measurement of NF- κ B (p65 subunit) transcriptional activity. (Inset) NF- κ B activating proteins were analyzed by immunoblotting. (B) MDA-MB-231 breast cancer cells were pretreated for 24 h with vehicle or the indicated inhibitors. Viable cells able to migrate through Matrigel over a 20-h period were stained with crystal violet and visualized by phase contrast microscopy. Invading cells were quantified and data graphed. (C) MDA-MB-231 breast cancer cells were treated for 24 h with the indicated concentrations of PU-H71, and protein extracts were subjected to immunoblotting.

(23, 24). Confirming of a similar premetastatic effect in TNBC, inhibitors of ERK2, Tyk2, and PKC α/β significantly inhibited migration of MDA-MB-231 cells (Fig. 3B). PU-H71, which induced the parallel degradation of these activated proteins (Fig. 3C), as well as potently suppressed NF- κ B activity (Fig. 3A), markedly contained MDA-MB-231 cell invasion, with 90% suppression at 1 μ M (Fig. 3B). Previous reports indicate that short-term treatment of breast cancer cells with GM and 17-AAG leads to transient activation of Akt and ERK observed as early as at 15 min and retained up to 4 h (25). Through this effect, these Hsp90 inhibitors are believed to increase the metastatic potential of cancer cells (25). In contrast, under similar conditions, PU-H71 potently inactivated both ERK1/2 and Akt (Fig. S4c).

Collectively, our findings suggest that a multitude of TNBC malignancy driving proteins, including those involved in proliferation, cell cycle progression, anti-apoptotic potential and invasion, interact with Hsp90 complexes that are recognized by PU-H71. In conclusion, the pluripotent effect of PU-H71 in TNBC cells is highly connected to its ability to inactivate these complexes in a parallel fashion, leading to downregulation of a large number of cancer-activating molecules.

PU-H71 Is Retained at Pharmacological Doses for Over 48 h in TNBC Tumors and Induces Extended Intratumoral Apoptosis and Depletion of Malignancy Driving Proteins.

To investigate whether Hsp90 may be efficiently modulated in vivo by PU-H71, we first evaluated the pharmacokinetic (PK) and pharmacodynamic (PD) profile of this agent in an MDA-MB-468 xenograft mouse model (Fig. 4 and Fig. S8). Pharmacologically relevant doses of PU-H71 rapidly reached tumors (Fig. S8b) and were retained at 48 h postadministration, with 10.5 and 1.8 μ g/g detected at 6 and 48 h, respectively (estimated as 20.6 and 3.6 μ M) (Fig. 4A); drug concentrations in nontumorous tissues and plasma declined rapidly, being almost undetectable by 6 h (Fig. 4A, Fig. S8 a and b). Because treatment of cultured MDA-MB-468 cells with 2.5 μ M PU-H71 for 48 h elicited death in 80–90% of cancer cells (Fig. S2a), it is reasonable to assume that the 3.6 μ M concentration of PU-H71 detected in tumors at 48 h, is a dose of high toxicity to tumors. Accordingly, high intratumoral

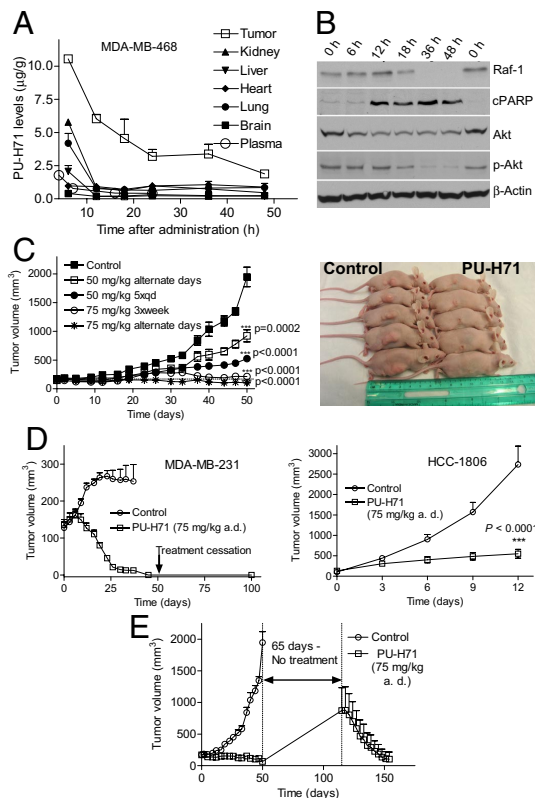


Fig. 4. PU-H71 leads to intratumor accumulation, extended down-regulation of anti-tumor driving molecules, and complete and retained responses at non-toxic doses. (A and B) MDA-MB-468 tumor-bearing mice were administered i.p. (i.p.) 1 dose of PU-H71 (75 mg/kg) dissolved in PBS pH 7.4. Animals were killed at the indicated times postadministration, and tumors and organs were harvested. (A) Levels of PU-H71 in tumors and the indicated organs were evaluated using high-performance liquid chromatography-tandem mass spectrometry (HPLC-MS/MS). Each data point represents the average value recorded from 2 individual mice. (B) Protein extracts from tumors were subjected to western blot analysis. (C) Mice (n = 8) bearing MDA-MB-468 subcutaneous (s.c.) xenografted tumors that reached a volume of approximately 100–200 mm³, were administered i.p. PU-H71 or vehicle at the indicated doses and schedules. (Left) Tumor volume (mm³) was estimated from caliper measurements. (Right) Photograph of representative MDA-MB-468 xenograft tumor mice from the control and treated (75 mg/kg PU-H71 a.d.) arms at 50 days into treatment. (D) Tumor volume measurements of MDA-MB-231 (Left) and HCC-1806 (Right) xenograft tumors (n = 8) treated i.p. with 75 mg/kg PU-H71 on an alternate day schedule. (E) Tumor volume measurements of MDA-MB-468 xenograft tumors (n = 8) treated i.p. with 75 mg/kg PU-H71 on an a.d. schedule. Treatment stopped 50 days after its inception and resumed 65 days later.

PARP cleavage, as well as sustained downregulation of Hsp90 clients was evident at this time point (Fig. 4B and Fig. S8c).

It was reported that while 17-DMAG appeared very potent in TNBC cells in vitro and abrogated onco-kinase Raf-1 expression in cultured MDA-MB-231 cells, i.v. administration of 75 mg/kg 17-DMAG to mice bearing MDA-MB-231 xenografted tumors had only minimal effect on Raf-1, with 20% reduction recorded at 24 h postadministration (9, 10). In contrast, PU-H71 administered at similar doses abrogated the intra-tumoral Raf-1 and Akt proteins in this model (Fig. S8c, Right), as well as in MDA-MB-468 and HCC-1806 tumors (Fig. 4B and Fig. S8c, Left). These effects were sustained for 36 and 48 h postadministration of the drug. Collectively, these data suggest that tumor PU-H71 pharmacokinetics correlate with tumor Hsp90 pharmacodynamics.

Interestingly, 17-DMAG and other Hsp90 inhibitors currently in clinical evaluation are reported to result in a less favorable PD profile in xenografts, with Hsp90 onco-client proteins returning to the initial levels between 8 to 24 h postadministration (26–28).

Along these lines, we find that in most cancer cells, Hsp90 oncocoagents, such as Akt, return to initial levels at 48 h after 17-DMAG, but remain undetectable up to 72 h with PU-H71, suggesting that a more transient inhibition of Hsp90 by certain agents could account for their poorer PD profile when compared to PU-H71.

Inhibition of Hsp90 by PU-H71 in TNBC Tumors Results in Complete and Durable Responses. PU-H71 was administered to TNBC tumor bearing mice on the following doses and schedules: 50 mg/kg either on an alternate day schedule (a.d.) or daily, 5 times per week (qd \times 5), and 75 mg/kg a.d. or 3 times per week (3 \times week). Treatment continued for 50 days, at which time tumors in the control group (PBS, treated with vehicle alone) reached 2 cm in length (Fig. 4C), and mice were killed according to our animal protocol. No overt toxicity was observed in either treatment group during this period, as evidenced by a lack of change in animal weight, appetite, or posture (Fig. 4C, *Right*). Furthermore, no visible internal organ damage was detected at sacrifice upon gross inspection. Significant effects on tumor growth were observed on each dose and schedule (Fig. 4C, *Left*). The effects were maximal on the 75 mg/kg a.d. schedule, where most tumors regressed, and complete responses were noted in 50% of the mice. When administered at 75 mg/kg a.d. in the MDA-MB-231 model, the drug induced a 100% complete response (Fig. 4D, *Left*), and tumors were reduced to scar tissue after 37 days of treatment. PU-H71 administration was stopped 2 weeks thereafter, but mice were monitored for an additional 60 days, during which period no visible local tumor recurrence was observed (Fig. 4D, *Left*). In the fast growing HCC-1806 tumors, administration of 6 doses over a 12-day period resulted in significant tumor growth inhibition (TGI) (87%, $P < 0.001$) (Fig. 4D, *Right*).

TNBCs Retain Responsiveness to PU-H71. To investigate whether tumors remain responsive to PU-H71, we re-treated some tumors that re-grew following treatment with PU-H71 (Fig. 4E). We started with a mouse cohort ($n = 8$) bearing MDA-MB-468 tumors of 180, 162, 198, 141, 183, 228, 158, and 128 mm³ in volume. During a 50-day treatment period at the 75 mg/kg a.d. schedule, these volumes changed to 0, 0, 129, 209, 53, 0, 0, 151 mm³. Untreated, these tumors would have reached an average volume of 2,000 mm³ at 50 days. Tumor absence or reduction and scar tissue in the location of the initial tumor were evident in PU-H71-treated mice (Fig. 4C, *Right*). To test whether tumors remained responsive to PU-H71, we allowed these mice a treatment-free period of 65 days (Fig. 4E). Four tumors remained undetected by visual inspection suggesting a 50% sustained remission rate, whereas the rest re-grew and reached an average volume of 872 ± 805 mm³. Treatment resumed on these mice for an additional 40 days. All tumors regressed with a 100% response rate and were reduced to an average volume of 104 ± 249 mm³, an 88% regression in tumor volume as compared to the tumor size on day 115 when treatment was restarted (Fig. 4E). These results indicate a lack of resistance to PU-H71. In addition, these long-term treatment periods, on which each mouse received 45 doses of 75 mg/kg PU-H71 administered every other day, resulted in no deaths and no apparent toxicities. In contrast, 20 or 30 mg/kg of the Hsp90 inhibitor 17-DMAG administered i.p. daily for 3 days to tumor bearing mice were reported to induce significant weight loss, diarrhea, and 23% toxic deaths (9, 10).

PU-H71 Is Nontoxic in Vivo. A more extensive toxicity study was performed in B6D2F1 mice, where animals received 50 and 75 mg/kg PU-H71 3 \times week for 21 days (13 males and 13 females/group). No evidence of macroscopic toxicity (weight, posture, fur, etc.) or microscopic toxicity was observed upon histologic examination of all vital tissues of PU-H71-treated mice (Fig. S9a and b). Additionally, there was no evidence of hematologic, renal, or hepatic toxicity as determined by blood cell counts, blood chemistries, liver function tests, and thyroid hormone levels (important

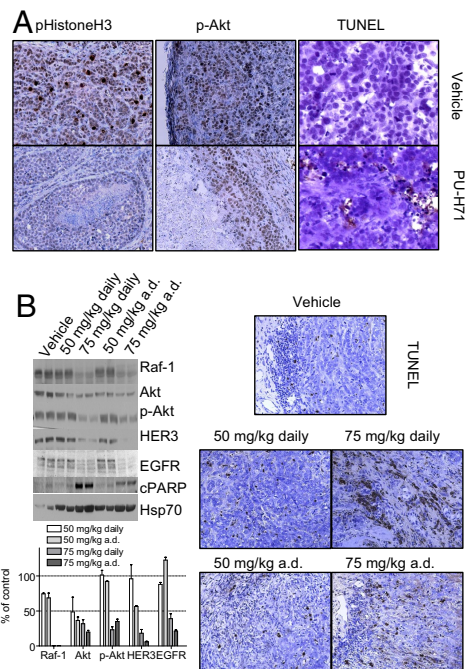


Fig. 5. Anti-tumor effects of PU-H71 are associated with down-regulation of several Hsp90-regulated malignancy driving proteins. (A) Representative MDA-MB-468 tumors harvested at 50 days into treatment from the control (*Upper*) and the 75 mg/kg 3 \times week (*Lower*) arms at 12 h after the last administered dose, were extracted, fixed in formalin, and paraffin-embedded. Samples were immunostained for markers indicating tumor proliferation (p -HistoneH3), aggressiveness (Akt phosphorylation at Ser-473), and apoptosis (TUNEL). (B) Mice bearing MDA-MB-468 tumors were administered i.p. PU-H71 at the indicated doses and schedules for 2 weeks ($n = 2$ mice per dose and schedule). Mice were killed at 12 h after the last administered dose, and tumors were harvested. Protein extracts from tumors were subjected to western blot analysis (*Upper Left*), and changes in protein levels quantified by densitometry and data graphed (*Lower Left*). Representative tumors were fixed in formalin, paraffin-embedded, and immunostained for apoptosis (TUNEL) (*Right*).

since PU-H71 is iodinated) (Fig. S9c). In contrast, untoward side-effects were previously reported for the geldanamycin-based Hsp90 inhibitors, 17-AAG and 17-DMAG (9, 10, 29).

Anti-Tumor Effects of PU-H71 Are Associated with Potent Reduction in the Proliferative, Anti-Apoptotic, and Invasive Potential of TNBC Tumors. Tumors on the 75 mg/kg 3 \times week and vehicle-only treated arms were selected for immunohistochemical analyses and quantification of several molecular markers (Fig. 5A). On this schedule, a 96% inhibition of tumor growth was observed (Fig. 4C). Reduction in actively duplicating cells was observed in the PU-H71-treated tumors as evidenced by a significant decrease in the number and intensity of phospho-histone H3 positive cells ($7.3 \pm 2.2\%$ in control versus $2.9 \pm 2.6\%$ in treated tumors) (Fig. 5A). A noteworthy decrease in the number and intensity of p -Akt positive cells was additionally detected in the treated tumors. The number of tumor cells staining negative, low and high for p -Akt was $9.5 \pm 2\%$, $69.8 \pm 8.3\%$, and $20.5 \pm 6.6\%$ in control, and $28.75 \pm 4.2\%$, $68 \pm 9\%$, and $3 \pm 0.7\%$, respectively, in treated tumors. These effects were paralleled by induction of apoptosis as evidenced by TUNEL staining. The number of TUNEL-positive tumor cells was $1.8 \pm 0.8\%$ and $12.7 \pm 5\%$ for control and treated tumors, respectively. Collectively, these findings show that a 96% inhibition of tumor growth by PU-H71 was associated by a 60% reduction in tumor cell proliferation, an 85% decline in activated Akt associated with survival and high invasive potential, and a 6-fold increase in apoptosis. Together, these findings demonstrated that similarly to

in vitro, PU-H71 led in vivo to a major reduction in the proliferative, anti-apoptotic, and invasive potential of the TNBC tumors.

To investigate changes that occur at molecular level and are associated with these multimodal anti-tumor effects of PU-H71, we evaluated the outcome of dose and schedule on several TNBC tumor molecular markers (Fig. 5B). Complete anti-tumor responses and tumor regressions, achieved at a dose of 75 mg/kg administered on an a.d. schedule, were associated with reduction in many proliferative and anti-apoptotic molecules, namely an 80%, 95%, 99%, 80%, and 65% decrease in EGFR, HER3, Raf-1, Akt, and p-Akt, respectively. Concordantly, significant intratumoral apoptosis, as evidenced by PARP cleavage (Fig. 5B) and TUNEL staining (Fig. 5C) was also noted. In contrast, moderate reduction in these molecular markers, especially when not associated with p-Akt depletion (Fig. 5B), resulted only in partial anti-tumor response, namely delay in tumor growth (Fig. 4C), and reduced apoptosis (Fig. 5B). Elevation in Hsp70 levels, a major anti-apoptotic molecule (30), was also observed, potentially limiting the magnitude apoptosis could be induced in vivo by PU-H71 (Fig. 5B).

In conclusion, our results show the true extent to which Hsp90 is an outstanding therapeutic target in TNBC, and PU-H71 delivers the most potent targeted single agent anti-tumor effect yet reported preclinically in this tumor type.

We used PU-H71 as an investigational tool to show that complete responses are possible preclinically in molecularly heterogeneous TNBC tumors with single agent administration of an Hsp90 inhibitor. Our data recorded with PU-H71 suggest that the variable performance of other Hsp90 inhibitors in TNBC tumors may not be explained by a decreased reliance of these tumors on Hsp90 and that other factors pertaining to the inhibitors themselves and not the target, are accountable.

Contrary to strategies that strike the TNBC cells only on a particular protein or signaling pathway they modulate, the potent efficacy of PU-H71 is likely due to its ability to inhibit, both in vitro and in vivo, Hsp90 that is bound to many proteins critical for the malignant phenotype of TNBC. Through this effect, PU-H71 leads to parallel destabilization and degradation of several key TNBC oncoproteins, many with roles in proliferation, anti-apoptotic potential, and metastasis. These conclusions are supported by our in vitro experiments showing complex formation of PU-H71-bound

Hsp90 with many of these proteins, as well as in vivo experiments that demonstrate that the magnitude of the anti-tumor response is dictated by and is concordant with sustained inactivation and down-regulation of multiple key Hsp90-dependent tumor-driving molecules by PU-H71.

Clinical trials of PU-H71 would be expected to maximally reveal the impact of Hsp90-targeted therapy in this disease. In addition, inhibitors targeting individual clients or pathways down-regulated by PU-H71 are currently in clinical evaluation providing an understanding for their distinct contribution to disease. These studies will also provide grounds for development of rational drug combinations incorporating PU-H71 and the individual agent, with the goal of providing a most efficacious shut-down of malignancy in TNBC.

Materials and Methods

Biochemical and Cellular Assays. Inhibition of Hsp90 was determined by a competitive assay that measures binding to Hsp90 in cellular lysates. Cellular expression and phosphorylation of malignancy driving proteins was determined by immunoassay, and cellular proliferation was determined by using the CellTiter-Glo Luminescent Cell Viability Assay (Promega). Cell cycle analysis was carried out by flow cytometry upon propidium iodide staining. Apoptosis was analyzed by confocal microscopy upon staining with YO-PRO-1, Hoechst 33342, and MitoTracker red or acridine orange and ethidium bromide. The invasive potential of MDA-MB231 cell lines was measured using an in vitro Boyden chamber Matrigel invasion assay. Identification of TNBC-specific Hsp90 clients was performed by proteomic analyses. Details of the methods are described in *SI Materials and Methods*.

Tumor Xenografts. In vivo experiments were carried out under an Institutional Animal Care and Use Committee-approved protocol. Details of the methods are described in *SI Materials and Methods*.

Statistical Analysis. Data were analyzed by unpaired 2-tailed t tests as implemented in GraphPad Prism (version 4; GraphPad Software). Unless otherwise noted, data are presented as the mean \pm SD of duplicate or triplicate replicates. Error bars represent the SD of the mean. If a single panel is presented, data are representative of 2 individual experiments.

ACKNOWLEDGMENTS. This work was supported in part by the Manhasset Women's Coalition Against Breast Cancer (G.C.), the Byrne Fund, the Geoffrey Beene Cancer Research Center of Memorial Sloan-Kettering Cancer Center (MSKCC) (G.C.), the Susan G. Komen Breast Cancer Foundation (G.C.), the Translational and Integrative Medicine Research Fund of MSKCC (G.C.), Mr. William H. Goodwin and Mrs. Alice Goodwin and the Commonwealth Cancer Foundation for Research and the Experimental Therapeutics Center of MSKCC (G.C., E.C.-L., and C.C.C.), and the intramural program of the National Cancer Institute (A.I.R. and L.V.). We thank Danuta Zatorska for the synthesis of Hsp90 inhibitors.

1. Yehieli F, Moyano JV, Evans JR, Nielsen TO, Cryns VL (2006) Deconstructing the molecular portrait of basal-like breast cancer. *Trends Mol Med* 12:537–544.
2. Amend K, Hicks D, Ambrosone CB (2006) Breast cancer in African-American women: Differences in tumor biology from European-American women. *Cancer Res* 66:8327–8330.
3. Kang SP, Martel M, Harris LN (2008) Triple negative breast cancer: Current understanding of biology and treatment options. *Curr Opin Obstet Gynecol* 20:40–46.
4. Foulkes WD, et al. (2003) Germline BRCA1 mutations and a basal epithelial phenotype in breast cancer. *J Natl Cancer Inst* 95:1482–1485.
5. Beliakoff J, Whitesell L (2004) Hsp90: An emerging target for breast cancer therapy. *Anticancer Drugs* 15:651–662.
6. Workman P, Burrows F, Neckers L, Rosen N (2007) Drugging the cancer chaperone HSP90: Combinatorial therapeutic exploitation of oncogene addiction and tumor stress. *Ann N Y Acad Sci* 1113:202–216.
7. Modi S, et al. (2007) Combination of trastuzumab and tanespimycin (17-AAG, KOS-953) is safe and active in trastuzumab-refractory HER-2 overexpressing breast cancer: A phase I dose-escalation study. *J Clin Oncol* 25:5410–5417.
8. Münster PN, Srethapakdi M, Moasser MM, Rosen N (2001) Inhibition of heat shock protein 90 function by ansamycins causes the morphological and functional differentiation of breast cancer cells. *Cancer Res* 61:2945–2952.
9. Hollingshead M, et al. (2005) In vivo antitumor efficacy of 17-DMAG (17-dimethylamino-17-demethoxygeldanamycin hydrochloride), a water-soluble geldanamycin derivative. *Cancer Chemother Pharmacol* 56:115–125.
10. Eiseman JL, et al. (2005) Pharmacokinetics and pharmacodynamics of 17-demethoxy 17-[(2-dimethylamino)ethyl]amino]geldanamycin (17DMAG, NSC 707545) in C.B-17 SCID mice bearing MDA-MB-231 human breast cancer xenografts. *Cancer Chemother Pharmacol* 55:21–32.
11. Chiosis G, Kang Y, Sun W (2008) Discovery and development of purine-scaffold Hsp90 inhibitors. *Expert Opin Drug Disc* 3:99–114.
12. Hsieh AC, Moasser MM (2007) Targeting HER proteins in cancer therapy and the role of the non-target HER3. *Br J Cancer* 97:453–457.
13. van der Horst EH, Murgia M, Treder M, Ullrich A (1994) Anti-HER-3 MAbs inhibit HER-3-mediated signaling in breast cancer cell lines resistant to anti-HER-2 antibodies. *J Biol Chem* 269:24747–24755.
14. Vassilev LT, et al. (2006) Selective small-molecule inhibitor reveals critical mitotic functions of human CDK1. *Proc Natl Acad Sci USA* 103:10660–10665.
15. Fernandez Y, Espana L, Manas S, Fabra A, Sierra A (2000) Bcl-xL promotes metastasis of breast cancer cells by induction of cytokines resistance. *Cell Death Differ* 7:350–359.
16. Yang SP, Song ST, Song HI (2003) Advancements of antisense oligonucleotides in treatment of breast cancer. *Acta Pharmacol Sin* 24:289–295.
17. Liu W, Bagaitkar J, Watabe K (2007) Roles of AKT signal in breast cancer. *Front Biosci* 12:4011–4019.
18. Cienas J (2008) The potential role of Akt phosphorylation in human cancers. *Int J Biol Markers* 23:1–9.
19. Umemura S, et al. (2007) Increased phosphorylation of Akt in triple-negative breast cancers. *Cancer Sci* 98:1889–1892.
20. Nakshatri H, Bhat-Nakshatri P, Martin DA, Goulet RJ Jr, Sledge GW Jr (1997) Constitutive activation of NF- κ B during progression of breast cancer to hormone-independent growth. *Mol Cell Biol* 17:3629–3639.
21. Radisky DC, Bissell MJ (2008) NF- κ B links oestrogen receptor signalling and EMT. *Nat Cell Biol* 9:361–363.
22. Häcker H, Karin M (2006) Regulation and function of IKK and IKK-related kinase. *Sci STKE* 357:re13.
23. Ide H, et al. (2008) Tyk2 expression and its signaling enhances the invasiveness of prostate cancer cells. *Biochem Biophys Res Commun* 369:292–296.
24. Dudek AZ, et al. (2008) Protein kinase C-beta inhibitor enzastaurin (LY317615.HCl) enhances radiation control of murine breast cancer in an orthotopic model of bone metastasis. *Invest New Drugs* 26:13–24.
25. Koga F, et al. (2006) Hsp90 inhibition transiently activates Src kinase and promotes Src-dependent Akt and Erk activation. *Proc Natl Acad Sci USA* 103:11318–11322.
26. Solit DB, et al. (2002) 17-Allylamino-17-demethoxygeldanamycin induces the degradation of androgen receptor and HER-2/neu and inhibits the growth of prostate cancer xenografts. *Clin Cancer Res* 8:986–993.
27. Chandrapaty S, et al. (2008) SNX2112, a synthetic heat shock protein 90 inhibitor, has potent antitumor activity against HER kinase-dependent cancers. *Clin Cancer Res* 14:240–248.
28. Eccles SA, et al. (2008) NVP-AUY922: A novel heat shock protein 90 inhibitor active against xenograft tumor growth, angiogenesis, and metastasis. *Cancer Res* 68:2850–2860.
29. Glaze ER, et al. (2005) Preclinical toxicity of a geldanamycin analog, 17-(dimethylamino)ethylamino-17-demethoxygeldanamycin (17-DMAG), in rats and dogs: Potential clinical relevance. *Cancer Chemother Pharmacol* 56:637–647.
30. Brodsky JF, Chiosis G (2006) Hsp70 molecular chaperones: Emerging roles in human disease and identification of small molecule modulators. *Curr Top Med Chem* 6:1215–1225.